An integrated workflow for design-informed structural optimization

I.T. Amarasinghe[1]*, H.M.S.T. Herath[1],H.M.Y.C. Mallikarachchi[1],

[1]Department of Civil Engineering, University of Moratuwa, Moratuwa, SRI LANKA.

Abstract

Structural optimization has become an important tool in the field of Civil Engineering, but there is limited research done on structural optimization of specific structures and components. This research study looks at developing a workflow for the design and analysis of structures using structural optimization to reduce the weight and cost, while keeping it safe under critical loading conditions. The Solid Isotropic Microstructure with Penalization (SIMP) for intermediate densities method is used for the topology optimization process, considering the minimum compliance as the objective function and the volume fraction as the constraint. The wheel loader arm is selected to demonstrate this workflow and commercially available software Abaqus FEA and SOLIDWORKS is used. Topology optimization of the arm is conducted using different volume constraints to identify the most optimum geometry comparing maximum von Mises stress, displacement, and mass with the original design. After the completion of the topology optimization process, Computer-Aided Design models are generated and shape optimization is conducted considering the different manufacturing constraints. The final optimized model has approximately 20% reduction of mass compared to the original structure, while stresses, displacement and strains are kept within the allowable limits in accordance with codes of practice.

***Keywords*—** Topology optimization, Shape optimization, Finite Element Analysis, SIMP method, Static analysis, Wheel loader arm

Introduction

Over the last few decades, structural optimization has become an important tool in the design process of structures and components [1]. Structural optimization is the rational establishment of a structural design that is the best of all possible designs within a prescribed objective and given set of limitations[2]. By optimizing a structure, it is possible to make various structures and components under specified constraints, as functional and economical as possible.

Structural optimization is considered to be of three main categories as shown in Figure 1. These are; size, shape and topology optimization. In size and shape optimization, the physical size of the members and the geometric layout are adjusted respectively, to minimize compliance. Topology optimization adjusts the internal configuration of the structure and members or parts of the structure will be deleted and a new layout will be prepared [3]. Among the three optimization categories, topology optimization is the most general form of structural optimization.

The general form of an optimization problem consists of three main elements to be considered. The objective function, design variable(s) and constraints. This is shown in Eq. (1) - (3),

$$\min_{\rho} : c = c(u(\rho), \rho) = \int_{\Omega} (u(\rho), \rho)\, dV \tag{1}$$

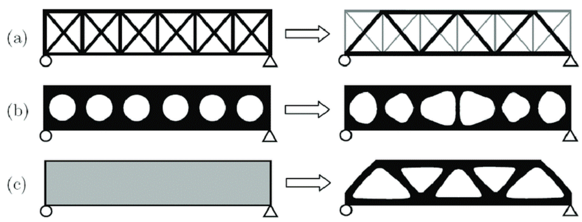

Figure 1: *Structural optimization categories (a) Size optimization (b) Shape optimization (c) Topology optimization (Reprinted from [4])*

$$\text{subject to } G_0(\rho) = \int_{\Omega} \rho dV - V_0 \leq 0 \tag{2}$$

$$G_j(u(\rho), \rho) \leq 0 \text{ with } j = 1, \ldots, m \tag{3}$$

Where c is the objective function, u is a state field that satisfies the linear or nonlinear linear state equations and ρ is the point-wise density of the material. If material is present, it is indicated by $\rho = 1$ and if there is a void it is indicated as $\rho = 0$. Ω represents the design space. Constraints are represented by G_j and m number of constraints are specified. V and V_0 represent the material volume and the design domain volumes, respectively.

c looks at the quantity that needs to be minimized for the best performance within Ω. Generally, the most used objective function is minimizing compliance [1]. During the optimization process we can enforce certain characteristics the solution must satisfy. For example, we can specify the maximum amount

*Corresponding author: 170026b@uom.lk
Received: March 16, 2023, **Published:** October 06, 2023

of material to be distributed. These enforced values are termed constraints.

While there are many topology optimization techniques available, including approaches such as homogenization approach, level set method, phase-field method [5], and neural network-based prediction approaches [6, 7] this research will be focusing on the density-based - Solid Isotropic Microstructure with Penalization (SIMP) for intermediate densities method. This method is becoming preferable, due to its higher computational efficiency and robustness compared to other methods. Another advantage is that the SIMP method provides a sharp layout without intermediate densities which are easier to realize in industrial applications [8].

While structural optimization is often adopted extensively in fields such as automotive and aerospace engineering (Liu et al., 2018, Krishnapillai, 2020), the use of structural optimization conducted on specific structures and components in the field of civil engineering is relatively new. Recent studies conducted in the field of civil engineering to find optimum structures and components under different constraints have produced significant results [9, 10].

Studies on large construction machinery such as the excavator machine have also produced designs of components with significant mass reduction some even up to even 27% of the initial values without affecting the strength [11].

Commercially available software such as Abaqus FEA and SOLIDWORKS have the ability to perform structural optimization, but the incorporation of these in the design process in the field of civil engineering is limited.

Therefore, there exists a research gap on the possibility of incorporating commercially available software to conduct structural optimization of specific structures and components in the field of civil engineering. This research gap identified relates closely to the issue brought up by Mei & Wang [1] on the limited applicability of structural optimization algorithms in the field of civil engineering.

To address the research gap, this paper presents a workflow for the design and analysis of structures using structural optimisation to reduce the weight and cost, while keeping it safe under critical loading conditions. The proposed workflow consists of 8 main steps, and is illustrated in Figure 2.

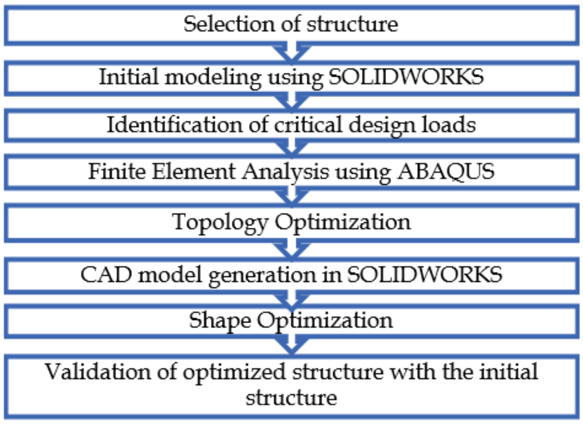

Figure 2: *Proposed workflow for structural optimization*

In this paper, the structure selected to demonstrate this workflow is the LK600A Kobelco wheel loader arm. While heavy construction machinery components have been optimized for load bearing, no thorough studies have been conducted under the avenues of structural optimization. By developing this method, the possibility of structural optimization of these structures can be explored and the same approach can be extended to all sort of other machinery.

Following the Introduction, Section 2 describes the structural idealization and numerical modeling conducted. Section 3 describes the topology optimization process followed. Section 4 discusses shape optimization followed by Section 5 which concludes the paper.

Structural idealization and numerical modeling

Critical Force Calculation

During the most critical working condition, two types of digging forces act on the wheel loader; the breakout force and the penetration force (Ozogan, 2020). The breakout force is created by the bucket and arm cylinder whereas the penetration or crowding force is generated by the traction force in the tires.

Breakout force is considered the maximum of the two forces; bucket curling force (FB) and the arm crowd force (FS). These forces are illustrated in Figure 3. For further details on these forces, readers are invited to refer to [12]. In this study, these forces are calculated according to the J1179 standard by the Society of Automotive Engineers (SAE). The weight of components and friction forces are to be excluded from these force calculations.

The maximum bucket curling force (F_0) is the digging force generated by the bucket cylinder. This was found to be 166.83 kN. Similarly, the maximum arm crowd force (F_s) is the digging force generated by the arm cylinder. This value was 44.78 kN. Therefore, the breakout force is considered as the maximum of these two values which was F_B with 166.83 kN.

The penetration force is generated by the traction forces in the tires ($F_t rac$). The tire traction breakaway equation is used [12] and a penetration force of 130.85

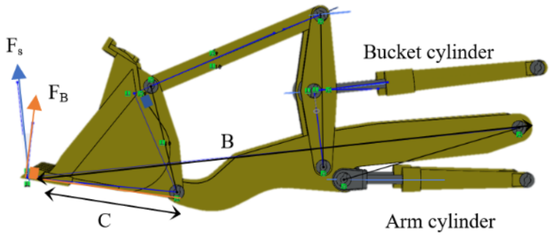

Figure 3: *Bucket curling force and arm crowd force*

kN is obtained.

Static Force Analysis

Surface Vehicle Standard J1179 states the critical forces acting on the wheel loader arm are the static forces acting during the digging action of the machine. Therefore, in this research, the dynamic effects such as inertial effects are not considered and a static force analysis was conducted. The material used for the wheel loader is considered as HARDOX 400 [11] and the material properties are presented in Table 1.

Table 1: *Material properties of HARDOX 400 steel [13]*

Material Property	Values
Density, $\rho_s teel$ (kg/m3)	8,000
Young's Modulus, E (N/mm2)	190,000
Poisson's ratio, ν	0.29
Yield Strength, σ_y (N/mm^2)	1,020

Figure 4(a) shows the free body diagram of the bucket and the attached rod. Considering equilibrium about the points X, Y, P, Q and considering the weights of the components W1, W2 and W3, the reactions at X and Y were calculated as illustrated in the figure. Subsequently, Figure 4(b) shows the free body diagram of the wheel loader arm. Considering the static equilibrium of the arm around the points X, Y, R, and the weight of the arm W4, the reactions at R and S were calculated as illustrated in the figure.

Finite Element Analysis

The initial model of the wheel loader arm was drawn using SOLIDWORKS and directly imported into Abaqus FEA for the finite element analysis. A mesh sensitivity analysis was conducted considering the total strain energy and the optimum mesh size was obtained was 30 mm at convergence. The forces and boundary conditions are applied to the original structure of the wheel loader arm. Horizontal and vertical forces were applied as concentrated forces at

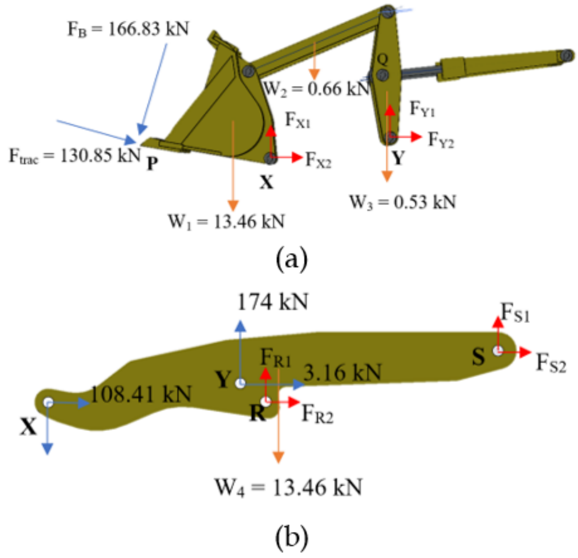

Figure 4: *Free body diagram of (a) the bucket and the attached rod (b) the arm*

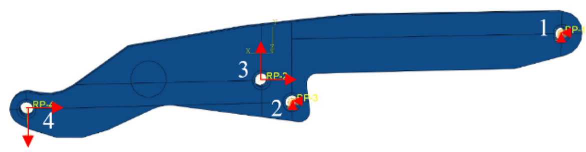

Figure 5: *Loads and boundary conditions on the wheel loader arm*

each reference point for nodes 3 and 4, and translational movements are restricted for nodes 1 and 2 as illustrated in Figure 5.

Based on the finite element simulation, the von Mises stress distribution obtained is illustrated in Figure 6. Eq. (4) indicates the allowable design stress for ductile materials,

$$\sigma_{\text{VM}} \leq \frac{\sigma_y}{\text{Safety Factor}} \tag{4}$$

where σ_{VM} is the maximum von Mises stress in the model and σ_V is the yield stress of the material. By taking the safety factor as 2 [11], the maximum von Mises stress needs to be below 510 MPa. The maximum stress obtained (361.7 MPa) for the finite element analysis is below this value, therefore the structure is safe in terms of stresses.

Similarly, the displacement distribution illustrated in Figure 7 is obtained and the maximum displacement of the arm was found as 10.76 mm. The maximum allowable value for the displacement is considered as the minimum thickness of the steel plate (Raghu et al., 2020). For this study, the maximum thickness of the plate is 60 mm, and therefore the maximum displacement is within the permissible limits.

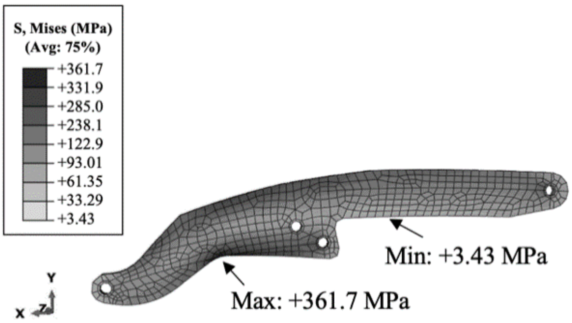

Figure 6: *Von Mises stress distribution from the Finite Element Analysis*

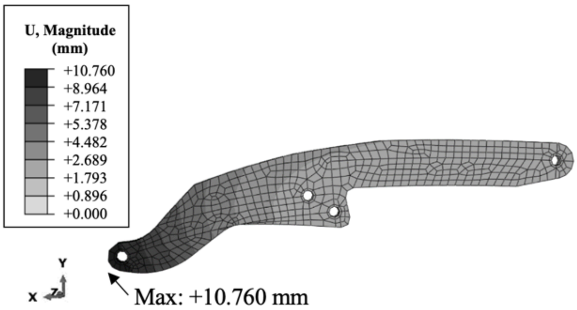

Figure 7: *Displacement distribution from the Finite Element Analysis*

Topology optimization process

In this study, the SIMP method is used for the topology optimization process, to find a minimum compliance design, based on the boundary conditions and forces being applied to the wheel loader arm.

SIMP Method

The SIMP method, [4] is becoming a widely used technique for topology optimization. This method uses a penalization factor to achieve density values closer to the lower and upper bounds of the design variables. The relation between the density design variable and the material property is given in Eq. (5),

$$E(\rho_i) = g(\rho_i)E_0 = \rho_i^p E_0 \tag{5}$$

where E_0 is the Young's Modulus of the solid material and p is the penalization factor. For this study, a penalization factor of 3 is used [8].

Objective Function, Variables and Constraints

Using the SIMP method, the topology optimization problem can be described as Eq. (6)-(9).

$$\min_{\rho} : c(\rho) = U^T K U = \sum_{e=1}^{N} (\rho)^p u_e^T k_e u \tag{6}$$

$$\text{subject to: } \frac{V(\rho)}{V_0} = f \tag{7}$$

$$KU = F \tag{8}$$

$$0 < \rho_{\min} \leq \rho \leq 1 \tag{9}$$

Here, ρ is the design variable that represents the relative density of each element. The objective function of this study is to minimize the overall compliance or in other words maximize the overall stiffness of the structure. Here, K is the total stiffness matrix, k_e is the element stiffness matrix. U is the displacement vector and F is the external force vector. Volume fraction denoted as f is given as the constraint with $V(x)$ and V_0 is the material volume and the design domain volume, respectively.

Topology Optimization of the Arm

Initially, the design domain of the wheel loader arm is defined. Some areas of the model including the area of one arm are connected to the other by the means of a cylindrical rod, and the sub-domains cannot be changed. These areas are called the non-design domain.

After assigning strain energy response as "minimizing the strain energy", an initial attempt was conducted for the topology optimization process using a volume fraction of 0.9. This initial optimization process converged at 14 cycles and the optimized geometry obtained showed a material reduction primarily in the middle of the arm.

It was observed that for this initial topology optimized model, the von Mises stress of the arm had slightly reduced overall compared to the result of the initial model with a maximum stress of 361.3 MPa. Similarly, the maximum defection had also reduced to 10.36 mm. Subsequently, the same process was carried out for different volume fractions.

Topology Optimization Results

Figure 8 shows the progressive removal of material for different volume fractions used.

As the volume fraction is reduced, a significant material reduction can be seen in the arm. The material removal follows the regions with the minimum stresses according to the results obtained during the initial finite element simulation of the original structure.

It should be noted that material removal between nodes 3 and 4 is limited (Refer to Figure 5 Loads and

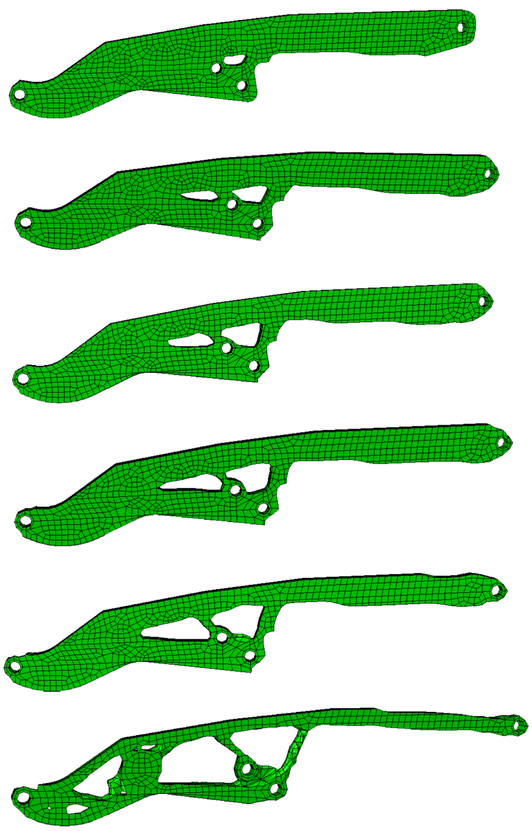

Figure 8: *Topology optimization results with various volume fractions f*

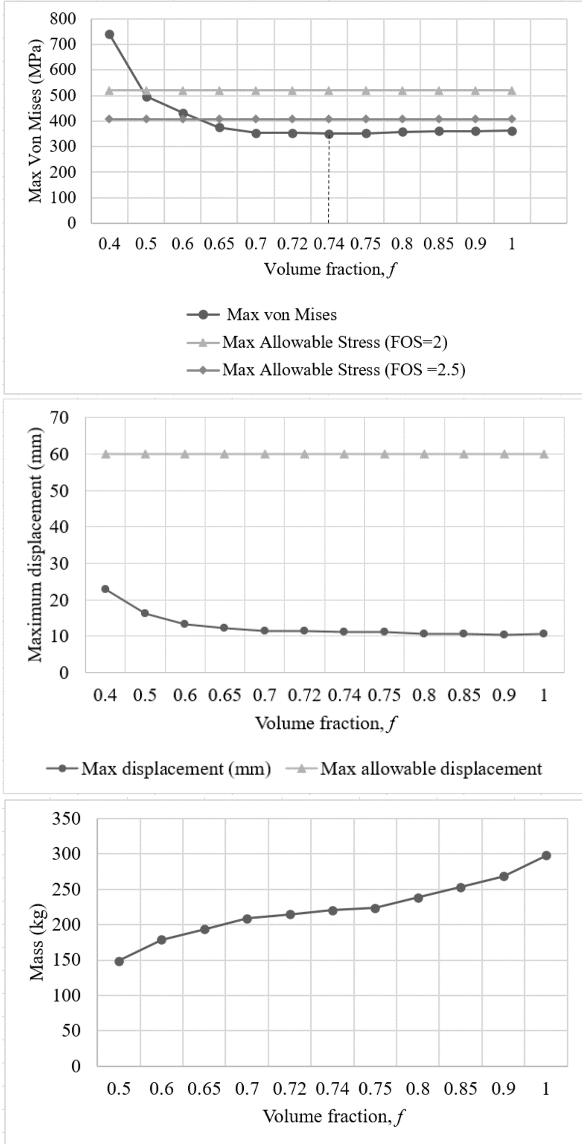

Figure 9: *Variation of (a) von Mises Stress, (b) Displacement, (c) Mass with volume fraction, f*

boundary conditions on the wheel loader arm for node numbers), and the removal can only be identified in a significant manner for volume fractions below 0.5.

Figure 9 illustrates stress and displacement variation with different volume fractions.

The optimization results show that the 0.74 volume fraction model features the most reduction in the maximum von Mises stress compared to the initial model. A Factor of Safety (FoS) of 2.5 has been used to further validate the allowable design stress of the arm, and whether the stresses are within the permissible limits. The displacement obtained from this model is 11.15 mm.

Considering the permissible limits of stress and displacement, a volume fraction below 0.5 will deem the structure to be unsafe. The 0.74 volume fraction model was considered the most optimum structure at this stage.

Shape optimization

The topology-optimized finite element models obtained from Abaqus FEA have complex geometries, which can be difficult for manufacturing purposes. Therefore, several constraints were considered with respect to manufacturability, and CAD models were created.

CAD Model Generation

The results obtained from the topology optimization process were exported from Abaqus FEA to SOLIDWORKS and used as guide geometries to determine where material should be removed from the arm, and the shapes and features are manually traced. One of the major geometric constraints to be considered when creating the CAD models is the distance between two openings in the arm.

Here, a minimum distance between the openings is considered as 0.3h, where *h_0* is the depth of the opening [14]. Another consideration is the sharp edges obtained through the topology optimization

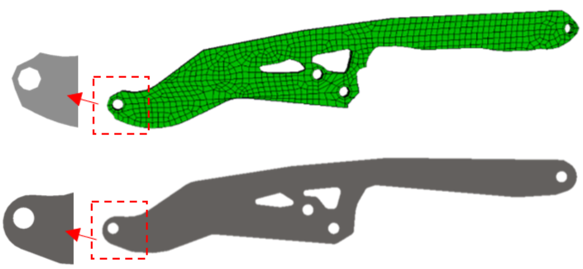

Figure 10: *(a) Topology optimized model obtained (b) CAD model generated*

iterations. These were rounded with fillets, with a minimum radius of 10 mm for ease of machining [13].

Figure 10 illustrates the CAD model created for the 0.74 volume fraction and its geometric comparison with the model generated in Abaqus FEA.

Static analysis was conducted on the CAD models using the same loading and boundary conditions as before, and the von Mises stresses, displacements, and strains were obtained.

It should be noted that one reason for the lack of application of topology optimization is the technical challenge faced during converting the optimized finite element models to CAD models to be used for manufacturing. Recently, studies are conducted to propose a fully automated and topologically accurate approach to synthesize a structurally-sound parametric CAD model from topology optimized finite element models [15, 16].

Final optimized structure

Table 2 shows the stresses, displacements, strains, mass and final volume fraction obtained from the analysis of four different optimized CAD models.

Therefore, the most optimum structure is that which gives a final volume fraction of 0.79, in terms of maximum stress and strain.

The comparison between the initial structure and the final optimized structure is illustrated in Table 3.

The maximum von Mises stress and the maximum displacement of the optimized arm are within the permissible limits. The maximum stress/strain ratio at the location with the maximum strain in the optimized arm is 175824 MPa, which is also within the permissible limits. The mass of the final model is 60.5 kg less than the mass of the original which is a 20.3% mass reduction.

The geometric model comparing the initial arm and the final optimized geometry is shown in Figure 11.

Table 2: *Comparison between the initial and the optimized arm*

	Initial Arm	**Optimized Arm**	**Difference**
Mass (kg)	298	237.5	-20.30%
Maximum von Mises stress (MPa)	362	359	-0.80%
Maximum displacement (mm)	10.76	9.57	-11.10%
Maximum strain	0.0016	0.0018	15.70%

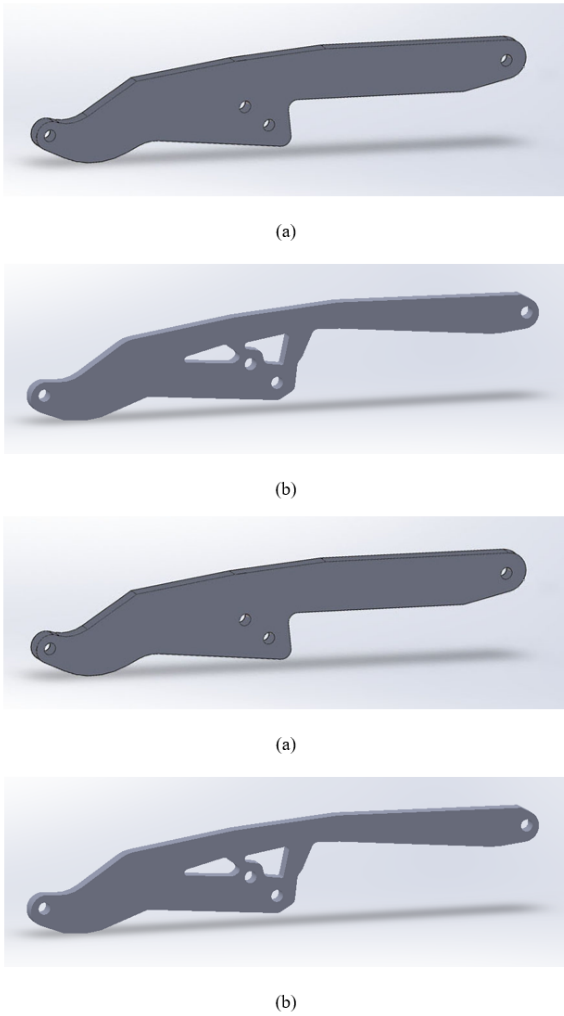

Figure 11: *a) Initial arm (b) Final optimized arm*

Conclusion and future work

Table 3: *Optimized results*

Initial f	Max stress (MPa)	Max displacement (mm)	Maximum strain	Mass reduction (%)	Final f
0.74	378	9.3	0.0021	13.5	0.84
0.72	362	9.34	0.00184	14.3	0.83
0.7	359	9.57	0.00182	20.3	0.79
0.65	364	9.61	0.00186	26.9	0.73

In this study, a workflow for the design and analysis of structures using structural optimization is proposed, taking a wheel loader arm as the application. Initially, the critical load calculation and the static force analysis of the wheel loader arm, as per the SAE J1179, were conducted. The respective forces and idealized boundary conditions were used in finite element modelling and model verification for stiffness, stability and strength. The SIMP-based topology optimization in Abaqus FEA software was subsequently used in the systematic optimization of the wheel loader arm by varying the volume fraction. The volume fraction of 0.75 yielded the optimal topology and achieved the best structural integrity. The pixelated output from Abaqus was post-processed in a CAD software to obtain the optimal ready-to-manufacture design. The final wheel loader arm CAD model attained a mass reduction of 20.3% compared to the original structure. This optimal structure satisfied all required design criterion in terms of strength, stiffness and stability. The proposed workflow could be used in the optimization of mechanical or structural components where noteworthy material savings could be achieved.

However, there are a few limitations in the scope of this research that need to be considered in future studies. Although this study did not consider the dynamic effects as per SAE J1179, it is recommended to consider other effects apart from static forces in future works. Another consideration that needs to be looked at is the fatigue of structural components during operation and the 3D nature of the forces acting on the components, including different angles of forces.

References

[1] Linfeng Mei and Qian Wang. "Structural Optimization in Civil Engineering: A Literature Review". In: *Buildings* 11.2 (2021). ISSN: 2075-5309. DOI: 10.3390/buildings11020066. URL: https://www.mdpi.com/2075-5309/11/2/66.

[2] Niels Olhoff and JE Taylor. "On structural optimization". In: *Journal of Applied Mechanics* 50.4b (1983), pp. 1139–1151.

[3] Nikolai Vladimirovich Banichuk. *Introduction to optimization of structures*. Springer Science & Business Media, 2013.

[4] Martin P Bendsøe. "Optimal shape design as a material distribution problem". In: *Structural optimization* 1 (1989), pp. 193–202.

[5] Ole Sigmund and Kurt Maute. "Topology optimization approaches: A comparative review". In: *Structural and multidisciplinary optimization* 48.6 (2013), pp. 1031–1055.

[6] Sumudu Herath and Udith Haputhanthri. "Topologically optimal design and failure prediction using conditional generative adversarial networks". In: *International Journal for Numerical Methods in Engineering* 122.23 (2021), pp. 6867–6887.

[7] Sumudu Herath, Udith Haputhanthri, and Chinthaka Mallikarachchi. "Initial design of trusses using topology optimization in a deep learning environment". In: *2020 From Innovation to Impact (FITI)*. Vol. 1. IEEE. 2020, pp. 1–6.

[8] George Rozvany. "The SIMP method in topology optimization-theoretical background, advantages and new applications". In: *8th Symposium on Multidisciplinary Analysis and Optimization*. 2000, p. 4738.

[9] James J Kingman, Konstantinos Daniel Tsavdaridis, and Vassilli V Toropov. "Applications of topology optimization in structural engineering: High-rise buildings and steel components". In: *Jordan Journal of Civil Engineering* 159.3097 (2015), pp. 1–23.

[10] JJ del Coz Díaz et al. "Design and shape optimization of a new type of hollow concrete masonry block using the finite element method". In: *Engineering Structures* 33.1 (2011), pp. 1–9.

[11] Bhaveshkumar P Patel and Jagdish M Prajapati. "Structural optimization of mini hydraulic backhoe excavator attachment using FEA approach". In: *Machine design* 5.1 (2013), pp. 43–56.

[12] Metin Özdoğan and Hakkı Özdoğanb. "Digging forces of electric rope shovel (ers) and adjustments made for a better digging shovel having optimum dipper rake and tooth angles". In: *Intl. Black Sea mining & Tunneling Symposium*. 2016.

[13] Yu Liu et al. "An efficient structural optimization approach for the modular automotive body conceptual design". In: *Structural and Multidisciplinary Optimization* 58 (2018), pp. 1275–1289.

[14] RM Lawson and SJ Hicks. *Design of composite beams with large web openings: in accordance with Eurocodes and the UK National Annexes*. Steel Construction Institute, 2011.

[15] Ge Yin, Xiao Xiao, and Fehmi Cirak. "Topologically robust CAD model generation for structural optimisation". In: *Computer methods in applied mechanics and engineering* 369 (2020), p. 113102.

[16] S Lowhikan and HMST Herath. "Nothing is better than something–Perspective of Structural Optimization in Civil Engineering Applications". In: (2022).